Eur. Phys. J. B **13**, 731–736 (2000)

THE EUROPEAN PHYSICAL JOURNAL B

EDP Sciences

Magnetic interaction between coupled quantum dots

J. Kolehmainen, S.M. Reimann[a], M. Koskinen, and M. Manninen

University of Jyväskylä, Physics Department, PO Box 35, 40351 Jyväskylä, Finland

Received 17 February 1999 and Received in final form 1 June 1999

Abstract. We study the magnetic coupling in artificial molecules composed of two and four laterally coupled quantum dots. The electronic ground-state configurations of such systems are determined by applying current spin density functional theory which allows to include effects of magnetic fields. While the ground-state of a two-dot molecule with strong enough inter-dot coupling tends to be antiferromagnetic with respect to the spins of the single dot components, we find that a square lattice of four dots has a ferromagnetic ground state.

PACS. 71. Electronic structure – 73.20.Dx Electron states in low-dimensional structures (superlattices, quantum well structures and multilayers) – 85.30.Vw Low-dimensional quantum devices (quantum dots, quantum wires etc.)

1 Introduction

Different kinds of micro- and nanostructures are nowadays fabricated in many laboratories around the world. A very popular species among them are quantum dots, *i.e.* small electron islands: electrical gates on top of a semiconductor heterostructure or etching techniques allow a confinement of the two-dimensional electron gas which is controllable in size and shape. Many of the properties of such artificially fabricated finite quantum systems show analogies to atomic physics. For this reason, quantum dots are often referred to as "artificial atoms" [1]. Going one step further, one can imagine to combine two (or more) quantum dots to an artificial molecule. Such structures can easily be realized experimentally – for example by gating the dot such that only a small barriers separate the single dots from each other. Other possibilities to realize artificial molecules are vertical dot molecules [2,3]. Quantum dots or dot molecules are interesting as they are ideal objects to study the properties of finite quantum systems of interacting particles experimentally. Compared to their atomic or molecular counterparts, they furthermore have the advantage that their two-dimensionality allows the study of magnetic effects in very strong fields. Much recent research focussed on the measurement of addition energy spectra and their theoretical interpretation. Quantum dot molecules have been extensively investigated by many groups. Conductance and the Coulomb blockade of two lateral quantum dots connected by a quantum point contact (QPC) have been studied experimentally [4] and theoretically [5–7]. Several other experimental investigations pointed at the analogy of "artificial molecules" and "artificial crystals" [8].

[a] e-mail: `reimann@phys.jyu.fi`

Antiferromagnetic ordering of coupled quantum dots was observed by G. Burkard *et al.* [9]. They calculated the exchange energy between the spins of two coupled dots, each containing one electron, and found that the antiferromagnetic state changes to ferromagnetic with increasing magnetic field. According to them, this opens up the possibility to use coupled quantum dots as quantum gate devices operated by magnetic fields.

In this article, we examine the magnetic coupling between quantum dots confining a larger number of electrons and show that both ferromagnetic and antiferromagnetic ordering may occur in artificial molecules composed of two and four quantum dots. A spontaneous polarization is observed in the regions of the quantum point contacts combining two and four single-dot components. In magnetic fields the electrons can get localized in the region of the saddle barrier connecting the single dots.

2 A two-dot molecule

We model a quantum dot molecule composed of two single quantum dots by trapping $2N$ interacting electrons (which are restricted to move in the plane $\mathbf{r} = (x, y)$ and are subject to a magnetic field $\mathbf{B} = B\mathbf{e}_z$) in a suitably formed confining potential $V(\mathbf{r})$. Approximating the confinement of each single dot by a spherical Gaussian, the external potential for the double-dot molecule can then be written in the form

$$V(x,y) = \frac{1}{2} r_0^2 \omega_0^2 \Bigg\{ 1 - \mathrm{e}^{-\left(\frac{x+d/2}{r_0}\right)^2 - \left(\frac{y}{r_0}\right)^2} - \mathrm{e}^{-\left(\frac{x-d/2}{r_0}\right)^2 - \left(\frac{y}{r_0}\right)^2} \Bigg\} . \quad (1)$$

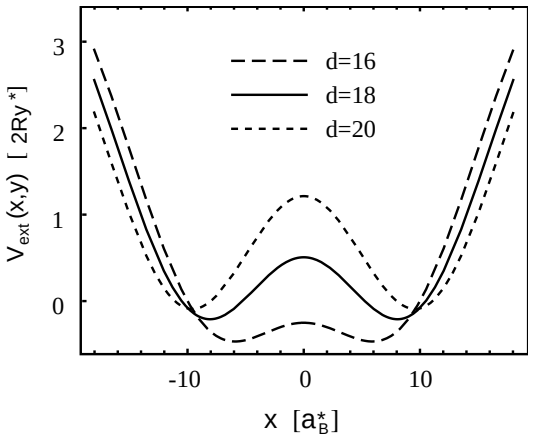

Fig. 1. External scalar potential $V(\mathbf{r})$ along the x-axis for $d = 16\,a_{\rm B}^*$, $d = 18\,a_{\rm B}^*$ and $d = 20\,a_{\rm B}^*$.

The value of r_0 determines the degree of harmonicity of $V(\mathbf{r})$ and together with the value of ω_0 defines the average electron density in the single-dot components. As the size of the single dots scales proportional to $\sqrt{N}$, we set $r_0 = \alpha\sqrt{N}$ and choose the scaling parameter α such that $r_0 = 10$ for $N = 10$. The average particle density of the dot, $n_0 = 1/(\pi r_{\rm s}^2)$, is determined by the two-dimensional Wigner-Seitz radius $r_{\rm s}$. We adjust the the strength $\omega_0^2 = e^2/(4\pi\epsilon_0\epsilon m^* r_{\rm s}^3\sqrt{N})$ of the external confinement such that n_0 is approximately constant in the single dots. The parameter d determines the distance between the centers of the two Gaussian potentials. (Due to the superposition of the Gaussians the distance between the two minima is actually slightly smaller than d.) Figure 1 shows the profile of the external potential along the x-axis for different dot-dot-distances.

The interaction between the electrons is the $1/r$ Coulomb interaction screened with the static dielectric constant ϵ of the material in question. To model the ground-state densities and energies of the many-electron system we apply the current spin density functional formalism (CSDFT) [10] which allows the inclusion of gauge fields in the energy functional. We perform the self-consistent calculations such that any restrictions in the spatial symmetries of the solutions are avoided. For a more detailed description of the numerical techniques we refer to Koskinen *et al.* [11]. We here only mention that the magnetic-field dependent exchange-correlation energy per particle was obtained from an interpolation between the Tanatar-Ceperley [12] results (generalized for intermediate polarizations) in zero fields and the parametrization for polarized electrons in the lowest Landau level by Fano and Ortolani [15]. More details are given in references [11,16].

The iterative solution of the Kohn-Sham equations results in different self-consistent solutions, corresponding to local minima in the potential energy surface of a free parameter space, as no symmetry restrictions were imposed. Thus, in order to find the ground state out of the possible self-consistent solutions, special care has to be taken in varying the initial conditions such that either antiferromagnetic or ferromagnetic coupling can be favored. In some cases we found it useful to fix the number of spin-up and spin-down electrons. In all cases, random perturbations were added to the initial potential.

2.1 Ground-state electronic structure of double-dot molecules

In the following, we first concentrate on two coupled dots with $10+10$, $12+12$ and $14+14$ electrons. (Here $N+N$ means that we have $2N$ electrons in the double dot system and on the average N electrons in each single dot.) We set the 2D density parameter to $r_{\rm s} = 1.51\,a_{\rm B}^*$, a value corresponding to the equilibrium density of the two-dimensional electron gas (which is actually very close to the value estimated in many experiments). The results will be given in effective atomic units with effective energies in $\mathrm{Ry}^* = m^* e^4/2\hbar^2(4\pi\epsilon_0\epsilon)^2$ and length units in Bohr radii, $a_{\rm B}^* = \hbar^2(4\pi\epsilon_0\epsilon)/m^* e^2$. Using the material parameters for GaAs, the effective mass is $m^* = 0.067\,m_e$, and the dielectric constant is $\varepsilon = 12.4$. Thus, one effective Rydberg corresponds to $\mathrm{Ry}^* = 5.93$ meV, and the effective Bohr radius equals $a_{\rm B}^* = 97.9$ Å. Then, one atomic unit of the effective magnetic field corresponds to $\mathrm{T}^* = 6.86$ T.

For the two-dot molecule we found it useful to define the total spin of the two single dots at both sides of the molecule separately as

$$S_{\rm dot} = \frac{1}{2}\int_{x>0} \mathrm{d}x \int \mathrm{d}y (n_\uparrow(\mathbf{r}) - n_\downarrow(\mathbf{r})), \qquad (2)$$

where $n_\uparrow$ and $n_\downarrow$ are the total spin up and spin down densities, respectively.

We first consider a two-dot artificial molecule containing $10 + 10$ electrons (without external magnetic field). Figure 2 shows the total electron density and the spin polarization for the antiferromagnetic ground state for four different values of the dot-dot distance d. A single 10–electron dot has total spin $S_{\rm dot} = \pm 1$ in its ground state. At distances between $d = 24$ and $d = 18\,a_{\rm B}^*$, the dots are almost separated and only very weakly coupled. The spin density of each dot can have a broken symmetry since the mean field reflects the internal symmetry of each dot [13,14].

With respect to the total spins in the single dot components of the dot molecule, $S_{\rm dot}$, their ground state is antiferromagnetic with $S_{\rm dot} = \pm 1.00$ for $d = 24$, $S_{\rm dot} = \pm 1.03$ for $d = 20$ and $S_{\rm dot} = \pm 1.08$ for $d = 18$. (Note that in the case of antiferromagnetic dot coupling the total spin in the each side need not to be an integer number). When the distance between the single dot components decreases to $d = 16\,a_{\rm B}^*$, *i.e.* the coupling between the single dots increases, the ground state remains antiferromagnetic but the total spin in each dot becomes smaller, being only $S_{\rm dot} = \pm 0.08$.

The double dot with the antiferromagnetic ground state (*i.e.* $S_{\rm dot,1} > 0$ and $S_{\rm dot,2} < 0$ or *vice versa*) has a ferromagnetic spin-isomer with a slightly higher total energy than the antiferromagnetic ground state. At $d = 18\,a_{\rm B}^*$

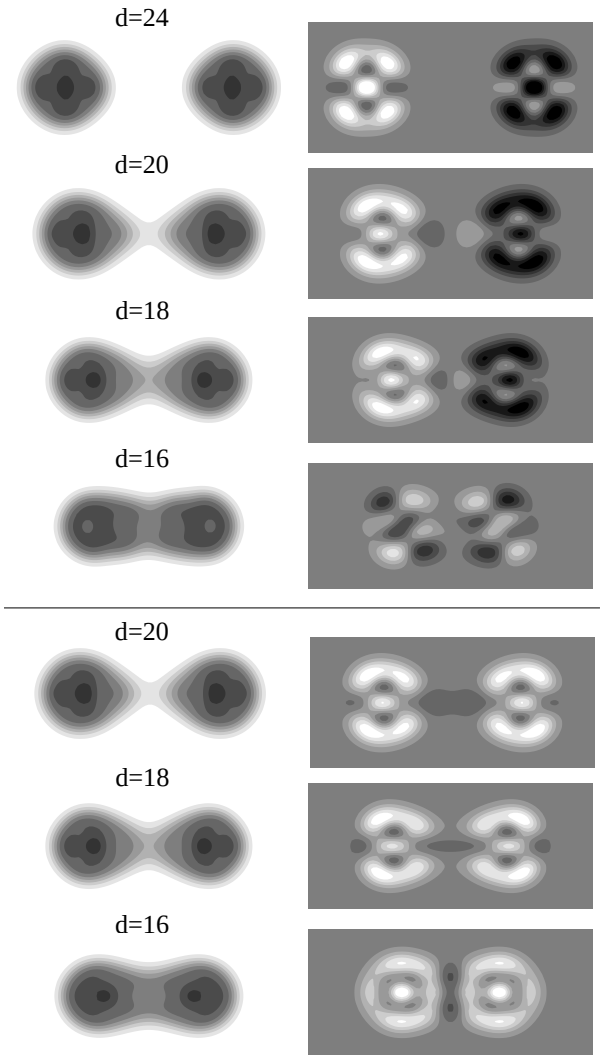

Fig. 2. Contours of the total density $n_\downarrow + n_\uparrow$ (left column) and spin density $n_\downarrow - n_\uparrow$ (right column) for coupled quantum dots with $10 + 10$ electrons and inter-dot distances $d = 16$, 18, 20 and $24\,a_{\rm B}^*$ (in zero magnetic field). (Dark (bright) gray-scales indicate maxima (minima). Note that the values of the density contours in the left and right column differ by a factor two).

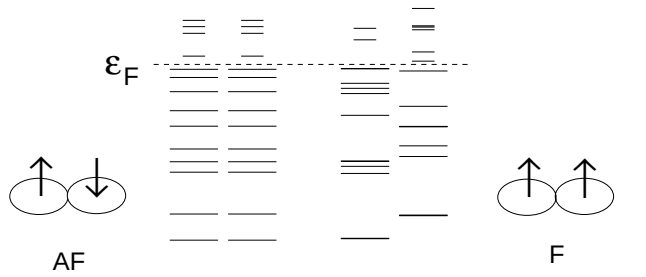

Fig. 3. Kohn-Sham energy eigenvalues of the antiferromagnetic (AF) ground state (left) and ferromagnetic (F) isomer (right) for a double-dot molecule with $10 + 10$ electrons and $d = 18\,a_{\rm B}^*$. (The dashed line indicates the Fermi energy $\varepsilon_{\rm F}$. The shorter lines indicate the lowest unoccupied states). The widths of the AF spectrum is 440 mRy* with a Fermi gap of 33.7 mRy*, while in the ferromagnetic case the Fermi gap is only 6.07 mRy*.

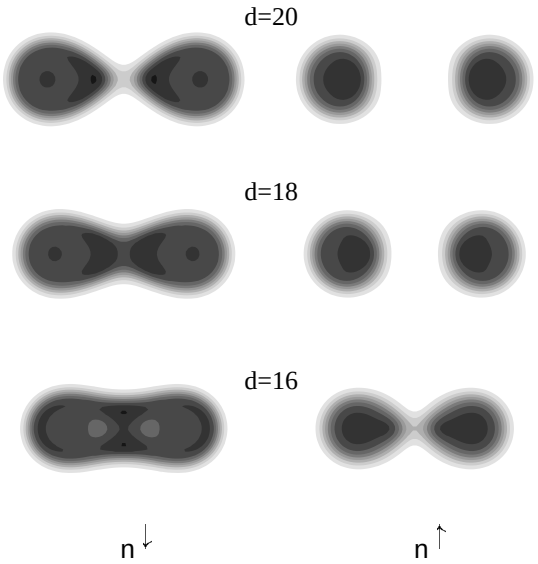

Fig. 4. Contours of spin down, spin up and total densities $n_\downarrow$, $n_\uparrow$ and n for coupled quantum dots with $10 + 10$ electrons and distances $d = 16$, 18, $20\,a_{\rm B}^*$ in a magnetic field of $B = 0.3$ T*.

this energy difference is 2.26 mRy*. It becomes smaller when the interdot distance increases, being only 0.33 mRy* for $d = 20\,a_{\rm B}^*$.

We should also mention that in the ferromagnetic configuration where the total spin of the dot molecule is $S_{\rm tot} = -2$ the spin-density at the area of the point contact between the two dots is positive, *i.e.* dominated by the minority spin.

Figure 3 shows the energy eigenvalues of the antiferromagnetic ground state and ferromagnetic isomer for $d = 18\,a_{\rm B}^*$. The antiferromagnetic state has a clearly larger Fermi gap which is the main reason that it is lower in energy.

Next, we apply a magnetic field to the $10 + 10$ dot molecule. For small field strength $B = 0.2$ T* the ground state electronic structure of the double dot was found to be fully paramagnetic, *i.e.* having $S_{\rm tot} = 0$ and identical densities $n^\downarrow = n^\uparrow$, for distances $d = 16$ and $18\,a_{\rm B}^*$ and if the distance of the dots is so large that they are fully decoupled. When at these $d-$values the field strength is raised to $B = 0.3$ T* the system becomes magnetized, having a total spin $S_{\rm tot} = -2$. Figure 4 shows the total density and the spin-up and spin-down densities as a function of the interdot distance. The density of the minority spin ($\uparrow$) is pushed away from the point-contact region which is dominated by the majority spin. At a magnetic field of $B = 0.5$ T* the system becomes fully polarized and forms two maximum density droplets which are weakly connected to each other. This behavior is in agreement with the phase transition to the maximum density droplet in circular dots [17,18]. In the case of a circular dot a further increase of the magnetic field will separate from

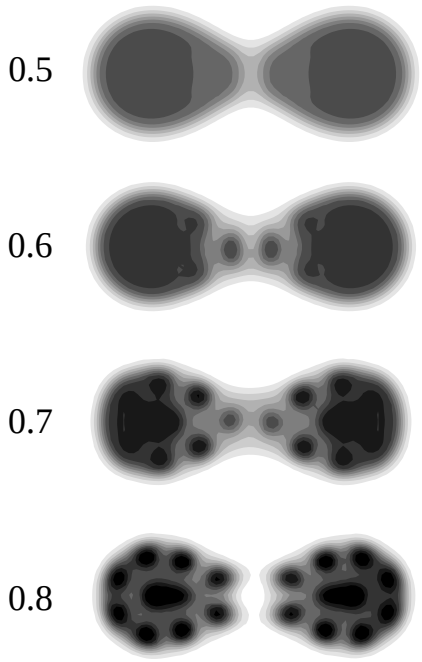

Fig. 5. Contours of total densities n for coupled quantum dots with $10 + 10$ electrons and interdot-distance $d = 18\,a_{\rm B}^*$ in magnetic fields $B = 0.5$, 0.6, 0.7 and 0.8 T*.

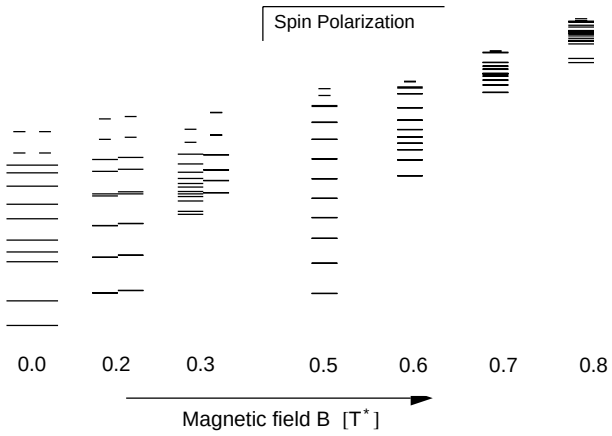

Fig. 6. Evolution of the single-particle spectra as a function of magnetic field for coupled dots with $10 + 10$ electrons and $d = 18\,a_{\rm B}^*$. The polarization transition occurs between $B = 0.4$ T* and 0.5 T*. (The shorter lines indicate the lowest unoccupied states.) The widths of the spectrum at $B = 0$ equals 440 mRy* with a Fermi gap of 33.7 mRy*.

the maximum density droplet a ring of electrons. In the unrestricted CSDFT this so-called Chamon-Wen [19] edge was found to have broken rotational symmetry and consists of localized electrons [16]. In the present case of a double dot the reconstruction of the maximum density droplet begins from the low-density region of the point contact. There the electron density starts to form strong maxima, each containing one electron. This is illustrated in Figure 5 where the electron density contours are shown as a function of the magnetic field. Figure 6 shows the evolution of the single particle spectrum as a function of magnetic field for $d = 18\,a_{\rm B}^*$. Note that in the case of a double dot each level is two-fold degenerate as we have one level in each dot. Only in the highest occupied levels this degeneracy is slightly split due to the interaction between the dots. Already at $B = 0.2$ T* the spectrum is drastically modified from the zero-field case due to level crossings, although the Zeeman splitting is still very small. At $B = 0.3$ T* the system gets partially polarized ($S_{\rm tot} = -2$). Then, at $B = 0.5$ T* after the polarization transition a maximum density droplet is formed, characterized by a rather regular spacing of the single particle levels. The localization of electrons at higher fields (0.7 and 0.8 T*) can be seen as a condensation of the levels into a very narrow band.

In order to see how the general trends depend on the electron number, we continue our studies for double dots with $12 + 12$ and $14 + 14$ electrons.

The single dot with 12 electrons has a full electronic shell and is non-magnetic with $S_{\rm dot} = 0$ [14]. Correspondingly, in zero field and at a large interdot-distance of $d = 20\,a_{\rm B}^*$, the double dot with $12 + 12$ electrons was found to be fully paramagnetic. At smaller distances, for these magic single-dot components no stable convergence could be obtained. However, when adding one more electron to the system, we found that this additional electron tends to be localized in the neck region, as it is energetically favorable to maintain the "magic" configuration of 12 electrons in each of the single dot components.

A 14–electron single dot has spin $S_{\rm dot} = 1$ [14]. Correspondingly, the $14 + 14$ dot with $d = 18$ at zero field becomes antiferromagnetic with respect to the spins in two weakly coupled single dots. In this case the integrated spin in each side is only $S_{\rm dot} = \pm 0.3$, but approaches $S_{\rm dot} = 1$ when the interdot distance increases.

In an external magnetic field of $B = 0.3$ T* both the $12 + 12$ and $14 + 14$ dots become magnetic with total spin $S = -2$ as in the case of the $10 + 10$ system. The densities are very similar to the results shown in Figure 5.

3 Four-dot molecule

The advantage of using inverted Gaussians to describe the external scalar potential of the quantum dots is that more complicated dot molecules can easily be constructed by a simple superposition of the external potentials of the single dots. Since the two-dot system prefers an antiferromagnetic coupling, it is now interesting to see whether a larger dot lattice also prefers antiferromagnetism with respect to the spins of the single dots forming the dot lattice. To this end we have studied a square and a row of four 10 electron dots and restricted our studies to the magnetic field-free case.

3.1 Four dots in a square

Contrary to the double dot, which favors antiferromagnetism, the square of four dots with $4N = 40$ has

a ferromagnetic ground state with a total spin $S_{\rm tot} = -4$. The antiferromagnetic state with $S_{\rm tot} = 0$ is clearly higher in energy. Figure 7 shows the electron densities and spin densities for these two states at interdot distances $d = 18\,a_{\rm B}^*$ and $d = 20\,a_{\rm B}^*$. The total electron density (see left column) is nearly independent of the magnetic coupling, but the internal structure of the spin-density in each dot (right column) depends slightly on the magnetic order. Figure 8 shows the single electron eigenvalues for the four dot square with interdot distance of $d = 18\,a_{\rm B}^*$. In the ferromagnetic case the Fermi gap is larger than in the antiferromagnetic case, leading to the preference of ferromagnetism.

3.2 Four dots in a row

Furthermore, we studied a linear row of four dots (with $4N = 40$ electrons) without an external magnetic field for an interdot distance of $d = 18\,a_{\rm B}^*$. Several magnetic isomers were obtained. The ground state was ferromagnetic but with a total spin $S_{\rm tot} = -3$ (and not $S_{\rm tot} = -4$ as one would expect in the light of the results discussed earlier). The Coulomb repulsion pushes the electron density slightly towards the end of the four-dot chain: the number of electrons in the end dots was 10.36 while it was 9.64 for the two dots in the center. The integrated spin at the end dots was $S_{\rm dot} = 0.95$ while it was $S_{\rm dot} = 0.55$ in the center dots. Two other magnetic isomers were obtained for the row of four dots. In both of them the total spin was zero. The total electron density was nearly identical to that of the ferromagnetic ground state. One of the isomers was an antiferromagnetic row with integrated spins of the different single dots as $S_{\rm dot} = -0.96$, 0.54, -0.54, and 0.96, *i.e.* very similar to those of the ferromagnetic row. In the other isomer, which energetically lies between the ferromagnetic and antiferromagnetic states, the sign of the spin changed in the middle of the row: the individual dots have spins $S_{\rm dot} = -0.85$, -0.41, 0.41, 0.85. Figure 9 shows the density and spin-density profiles for the three magnetic states. The total density is the same in each case. The results show that the magnetic coupling between many-electron dots is much more complicated than that of single-electron dots. In the Hubbard model in the limit of strong interaction one finds that antiferromagnetic coupling is favored [20], irrespective of the geometry of the dot molecule. In agreement with the Hubbard model results, the LSDA indeed gives antiferromagnetic order for the ground-state of four electrons in a four-dot molecule.

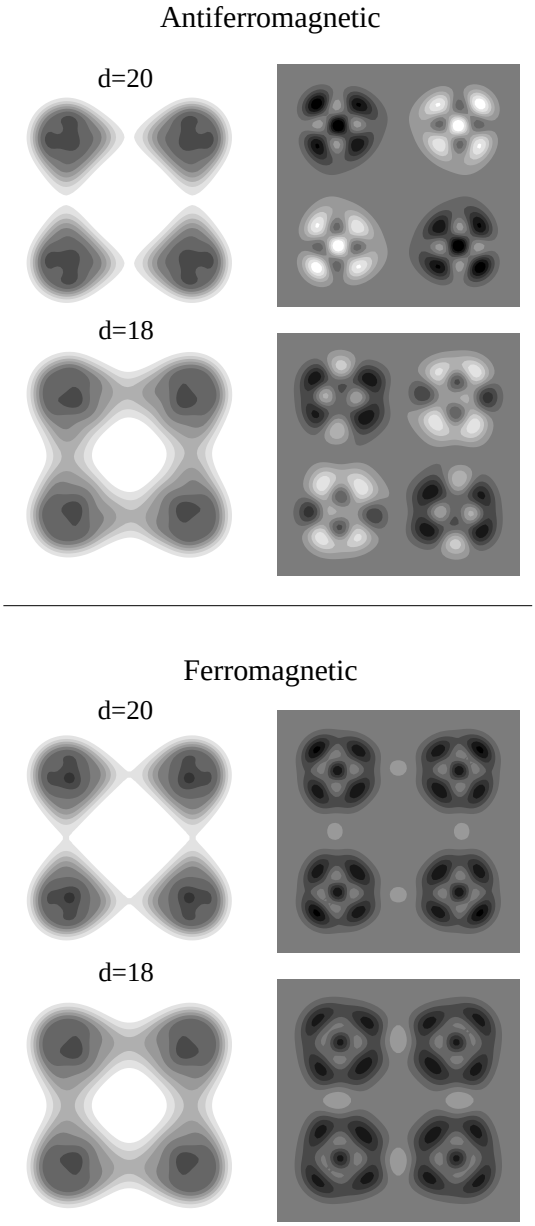

Fig. 7. Contours of the total densities $n_\downarrow + n_\uparrow$ (left column) and spin densities $n_\downarrow - n_\uparrow$ (right column) for a square of four coupled quantum dots with $10 + 10 + 10 + 10$ electrons, with nearest neighbor distances $d = 18$ and $d = 20\,a_{\rm B}^*$ (without magnetic field). (the upper (lower) panel shows the antiferromagnetic (ferromagnetic) state). (Dark (bright) gray-scales indicate maxima (minima) like in Fig. 2).

4 Conclusion

We have observed that when two quantum dots are weakly coupled to form a quantum dot dimer they seem to prefer an antiferromagnetic ground state. This is the case for the $10 + 10$ dot molecule, where in the single $N = 10$ dot the highest orbital is more than half full, as well as for the $N = 14$ dot where it is less than half full. Naturally, nonmagnetic dots ($N = 12$) form a nonmagnetic molecule.

In an external magnetic field the electronic structure changes already before the field exceeds a value where spin-polarization sets in. Increasing the magnetic field further, polarization starts at the low-density regimes in the neck region and proceeds until two nearly independent maximum density droplets are formed in both sides of the dot molecule. The properties of this state are independent of the number of electrons in each dot. At even higher fields the electrons start to localize like in the case

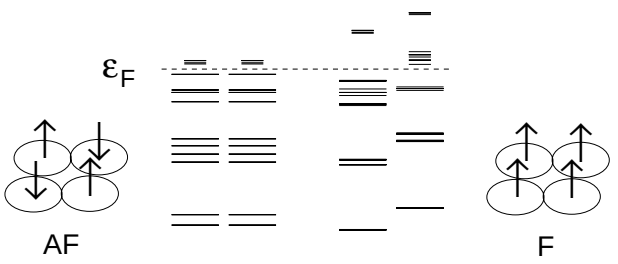

Fig. 8. Single-particle spectra of the antiferromagnetic (AF) isomer (left) and ferromagnetic (F) ground state (right) for a four-dot molecule with $4N = 40$ electrons and nearest neighbor distance $d = 18\,a_B^*$ (shorter lines indicate the lowest unoccupied states). The widths of the AF spectrum is 400 mRy* with a Fermi gap of 27.0 mRy*, while in the ferromagnetic case the Fermi gap of 42.2 mRy* is considerably larger.

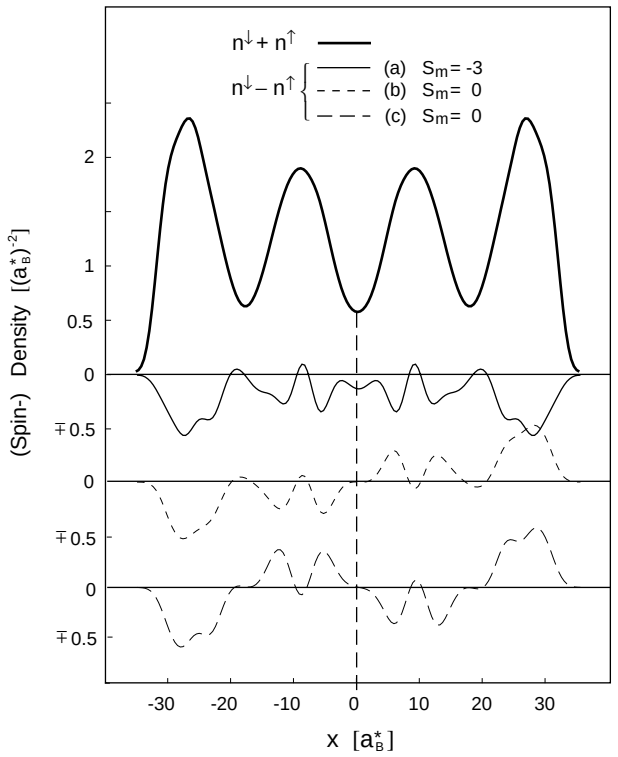

Fig. 9. Total densities $n_\downarrow + n_\uparrow$ and spin densities $n_\downarrow - n_\uparrow$ for a row of four coupled dots with $4N = 40$ electrons with interdot distance $d = 18\,a_B^*$, plotted along the x-axis.

of single dots [16]. In the double dot, however, this localization begins in the region of the neck between the two single dots, where the average electron density is lowest.

Surprisingly, in a square of four quantum dots with $4N = 40$ electrons the ground state without an external field is ferromagnetic and the antiferromagnetic state is higher in energy. Similarly, the row of four quantum dots has a ferromagnetic-like ground state. The total spin, however, was reduced by one due to the Coulomb repulsion which pushes the electron density slightly towards the ends of the row.

We conclude with the remark that the magnetic coupling in quantum dot molecules or lattices of several interacting quantum dots is rather complex. The examples studied above shed some light on the possible electronic ground state structures of two-and four-dot molecules. Much more work has to be done before general conclusions can be made.

This work was supported by the Academy of Finland and the TMR programme of the European Community under contract ERBFMBICT972405. We are grateful to Poul Erik Lindelof for initiating this study.

References

1. R. Ashoori, H.L. Störmer, J.S. Weiner, L.N. Pfeiffer, K.W. Baldwin, K.W. West, Phys. Rev. Lett. **71**, 613 (1993); R. Ashoori, Nature **379**, 413 (1996).
2. D.G. Austing *et al.*, Physica B **206**, 249 (1998).
3. S. Tarucha *et al.*, Physica E **3**, 112 (1998).
4. F.R. Waugh, M.J. Berry, D.J. Mar, R.M. Westervelt, K.L. Campman, A.C. Gossard, Phys. Rev. Lett. **75**, 705 (1995).
5. J.M. Golden, B.I. Halperin, Phys. Rev. B **53**, 3893 (1996).
6. K.A. Matveev, L.I. Glazman, H.U. Baranger, Phys. Rev. B **54**, 5637 (1996); K.A. Matveev, L.I. Glazman, H.U. Baranger, Phys. Rev. B **53**, 1034 (1996).
7. Y.-L. Liu, Phys. Rev. B. **56**, 6732 (1997).
8. R.H. Blick *et al.*, Phys. Rev. Lett. **80**, 4032 (1998); Phys. Rev. B **53**, 7899 (1996); N.C. van der Waart *et al.*, Phys. Rev. Lett. **74**, 4702 (1998); L. Kouwenhoven, Science **268**, 1440 (1995).
9. G. Burkard, D. Loss, D.P. DiVincenzo, `cond-mat/9808026` (1998).
10. G. Vignale, M. Rasolt, Phys. Rev. B **37**, 10685 (1988).
11. M. Koskinen, J. Kolehmainen, S.M. Reimann, J.Toivanen, M. Manninen, Eur. Phys. J. D **9**, 487 (1999).
12. B. Tanatar, D. M. Ceperley, Phys. Rev. B **39**, 5005 (1989).
13. We note that the self-consistent mean field approach can reflect the internal symmetry of the many-body state and refer to nuclear physics, where the mean-field approach can describe the internal shapes of nuclei, although in the laboratory frame of reference the nuclei are spherically symmetric.
14. M. Koskinen, M. Manninen, S.M. Reimann, Phys. Rev. Lett. **79**, 1389 (1997).
15. G. Fano, F. Ortolani, Phys. Rev. B **37**, 8179 (1987).
16. S.M. Reimann, M. Koskinen, M. Manninen, B.R. Mottelson, Phys. Rev. Lett. **83**, 3270 (1999).
17. A.H. McDonald, S.R. Eric Yang, M.D. Jonson, Aust. J. Phys. **46**, 345 (1993).
18. O. Klein, C. de Chamon, D. Tang, D.M. Abusch-Magder, U. Meirav, X.-G. Wen, M.A. Kastner, S.J. Wind, Phys. Rev. Lett. **74**, 785 (1995).
19. C. de Chamon, X.G. Wen, Phys. Rev. **49**, 8227 (1994).
20. E.B. Kolomeisky, J.P. Straley, Rev. Mod. Phys. **68**, 175 (1996); M. Manninen (unpublished).